Fingerprint Recognition Using Model-Based Density Map

Dingrui Wan and Jie Zhou, *Senior Member, IEEE*

***Abstract*—Utilizing more information other than minutiae is much helpful for large-scale fingerprint recognition applications. In this paper, we proposed a polynomial model to approximate the density map of fingerprints and used the model's parameters as a novel kind of feature for fingerprint representation. Thus, the density information can be utilized into the matching stage with a low additional storage cost. A decision-level fusion scheme is further used to combine the density map matching with conventional minutiae-based matching and experimental results showed a much better performance than using single minutiae-based matching.**

***Index Terms*—Decision fusion, density map, fingerprint recognition, polynomial approximation.**

I. Introduction

RECENTLY, biometric technologies have shown much more importance in various applications. Among them, fingerprint recognition is considered one of the most reliable and mature technologies and has been extensively used in personal identification. In recent years, this technology has received increasingly more attention [1]–[3], and the performance shows it is competent in applications on small databases; however, it is not satisfactory for large-scale applications [4].

Most classical fingerprint recognition algorithms [1]–[3], [5], [6] take the minutiae and the singular points, including their coordinates and direction, as the distinctive features to represent the fingerprint in the matching process. Then the minutiae feature is compared with the minutiae template; if the matching score exceeds a predefined threshold, these two fingerprints can be regarded as belonging to a same finger.

In [4], Jain *et al.* theoretically analyzed the performance's upper bound of minutiae-based fingerprint recognition. For example, the estimation of the probability that an imposter pair of fingerprints both containing 36 minutiae will match 12 minutiae is about 6.10×10^{-8}. It is also indicated that the performance would fall drastically with noise and false minutiae detection. In [7], Tan and Bhanu studied the individuality of the fingerprints by adding the ridge count information between different minutiae. Their conclusions show incorporating more discriminatory information can largely strengthen this scientific basis for fingerprint recognition. In [8] and [9], Jain *et al.* have proposed hybrid schemes by combining the minutiae with a novel feature called FingerCode, which is produced by applying a set of Gabor filters on the fingerprint. A better performance can be obtained by using these hybrid algorithms than singly using minutiae matching. In [10], a minutiae-descriptor has been proposed and some orientation-based information from the neighborhood of the minutiae points is added in the matching stage. Some researchers also tried to find some other features directly based on original fingerprint images. In [11], the authors proposed an image-based method by using integrated wavelet and Fourier–Mellin invariant transform (WFMT) feature.

A novel kind of features based on density map is considered in this paper. Density map is a set of ridge distance on each point in the fingerprint and the ridge distance is usually defined as the length of the segment connecting the centers of two adjacent and parallel ridges along the line perpendicular to the ridges (see Fig. 1 for an illustration of ridge distance). Obviously, density map describes the ridges' denseness or sparseness of a given fingerprint. In [12], it has been shown an important factor for fingerprint enhancement. In [13], a density map is proven as a key factor in synthetic fingerprint generation. These researches reveal that the density map plays an important role in fingerprint representation. That is the reason why we take the density map into account as a feature for fingerprint representation.

In this paper, we propose to use the density map as a novel feature for the fingerprints' representation. Since the density maps directly computed from the fingerprints lack in robustness against noise and distortion, a polynomial model is proposed to approximate the coarse density map, and this model can be regarded as an intuitive reflection of ridges' denseness and sparseness. Then, the model's parameters can be saved for further usage in fingerprint matching with a low additional storage cost. Because the modeled density map is a global representation, which complements with the minutiae, a local representation, a better performance can be obtained by fusing the results of density map matching with conventional minutiae-based matching.

This paper is organized as follows. Section II introduces the model-based density map and the approximation process. In Section III, an algorithm of fingerprint recognition combining minutiae and density map is described. Section IV gives the experimental results to evaluate the performance of the proposed algorithm. Section V summarizes the paper.

II. Model-Based Density Map Computation

Although the density map contains rich information, it is not suitable to directly use it in the recognition scheme due to its

Manuscript received June 23, 2004; revised August 2, 2005. This work was supported in part by the Natural Science Foundation of China under Grants 60205002 and 60332010, in part by the Natural Science Foundation of Beijing under Grant 4042020, and in part by the National 863 Hi-Tech Development Program of China under Grant 2001AA114190. The associate editor coordinating the review of this manuscript and approving it for publication was Dr. Gopal Pingali.

The authors are with Department of Automation, Tsinghua University, Beijing 100084, China (e-mail: wandingrui00@mails.tsinghua.edu.cn; jzhou@tsinghua.edu.cn).

Digital Object Identifier 10.1109/TIP.2006.873442

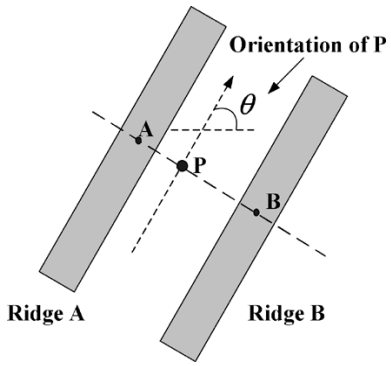

Fig. 1. Illustration of ridge distance. The distance between points A and B is the ridge distance at point P.

heavy storage cost. Another reason why we cannot use the density map directly is that it lacks in robustness against noise and distortion. Furthermore, the ridge distance in the vicinity of minutiae points and singular points usually changes sharply [see Fig. 4(e)], so we need to reduce the redundancy between density map and minutiae in order to utilize density map into conventional algorithms. Due to the above reasons, we propose to use a polynomial function with two variables for the approximation of the coarse density map.

The whole computation process of model-based density map mainly consists of the following steps: effective region estimation, orientation field estimation, fingerprint enhancement, coarse density map extraction, and weighted polynomial approximation (i.e., modeling). In Fig. 2, the flowchart of model-based density map computation is depicted.

A. Effective Region Estimation

The fingerprint image is divided into many blocks (whose size is 16×16 pixels). For each block, the variance of the gray levels is computed. If the value exceeds the predefined threshold, this block is regarded as an effective block. Combining all effective blocks together, some post-processing steps like dilation and erosion in mathematical morphology are taken based on some simple assumptions, such as the effective region is only one connected region and has no inner holes.

The effective region needs to be recorded for further usage in the matching stage. For live-scanner applications, a simple 16-point chain code is utilized for that. First, the center of the region is computed by averaging the x coordinate and y coordinate of all points in the effective region. Then, 16 lines are drawn from the center with 16 different angles, i.e., $0, \pi/8, \pi/4, \cdots, 7\pi/4$, and $15\pi/8$, respectively. The intersection point of each line with the region edge is recorded in turn. Thus, totally 32 bytes are needed for the storage of the chain code. See Fig. 3 for an illustration.

B. Orientation Field Estimation

Orientation field is defined as the local orientation of the ridges, which is important for fingerprint recognition. In this paper, we use a so-called model-based method for the computation of orientation field, which is proposed by one of us in [14]. First a combination model is established for the representation of the orientation field by considering its smoothness except for several singular points, in which a polynomial model is used to describe the orientation field globally and a point-charge model is taken to improve the accuracy locally at each singular point. When the coarse field is computed by using the gradient-based algorithm, a further result can be gained by using the model for a weighted approximation. Due to the global approximation, this model-based orientation field estimation algorithm has a robust performance.

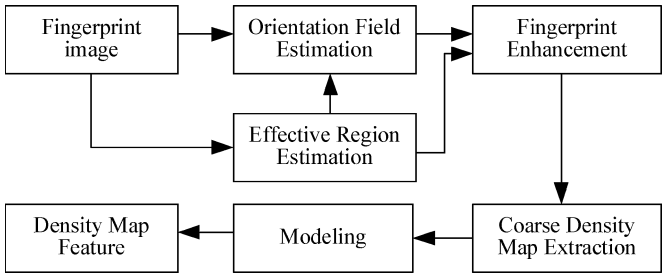

Fig. 2. Flow-chart of model-based density map computation.

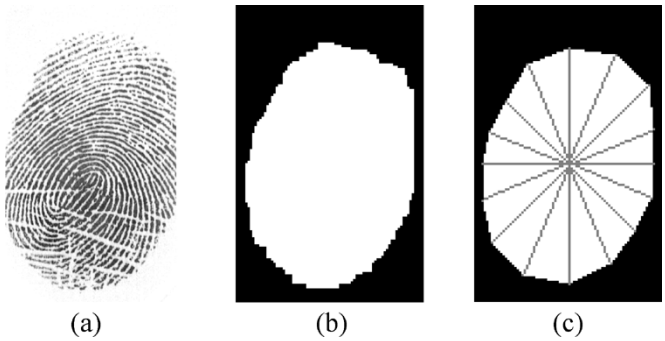

Fig. 3. Illustration of effective region estimation: (a) original fingerprint; (b) effective region computed directly; and (c) effective region represented with 16-point chain code.

C. Fingerprint Enhancement

The goal of fingerprint enhancement is to make the ridges clearer and reduce the noise's affect. The method used here is quite similar with that used in [5]. Since the gray-level values on ridges attain their local maxima along a direction normal to the local ridge orientation. Pixels can be identified to be ridge pixels based on this property. The fingerprint image is convolved with a matched Gabor-like filter, which is capable of adaptively accentuating the local maximum gray-level values along a direction normal to the local ridge orientation. Then a threshold can be easily chosen to segment the ridges adaptively [15].

D. Coarse Density Map Estimation

There are mainly two ways to compute coarse ridge distance [16]: One is spectral approach and the other one is the spatial approach. The former is robust to noise but also blur the ridge density information in those regions with high curvature (because the spectral response is obtained in a specified window and the high curvature pattern will obfuscate the two peaks in spectral domain). The latter works quite well after a suitable smooth post-processing, on the other hand, it has a lower computation cost. So, in our study, we choose the spatial approach to compute coarse density map.

To estimate the density on a given point, first, we binarize the enhanced image as the ridge map with a certain threshold, then, draw a line passing the given point with the direction perpendicular to the orientation of the given point; then detect the nearest two central points of two neighboring ridges on the line, and the distance between the two center points is regarded as the ridge distance on the given point.

E. Weighted Polynomial Approximation

We want to model the original density map by a polynomial with two variables. This bivariate polynomial can be computed by using the Weighted Least Square (WLS) algorithm [17]. The polynomial is written as

$$p(x,y) = \sum_{i=0}^{n}\sum_{j=0}^{n} a_{ij}x^i y^j \tag{1}$$

where n is the order of the polynomial. The coefficients of the polynomial can be obtained by minimizing the weighted square error between the polynomial and the coarse density map computed from the given fingerprint, i.e., minimizing the following function:

$$J = \sum_{k=1}^{K} w_k \left[z_k(x_k,y_k) - p(x_k,y_k)\right]^2 \tag{2}$$

where K denotes the number of samples, $z_k(x_k,y_k)$ is the density value at (x_k,y_k), and w_k is a weight factor on the point, (x_k,y_k). The selection of the weight factor will be discussed in the next paragraph. The variables in the above optimization problem are the parameters of the polynomial, $\{a_{ij}\}$. They can be computed by solving the following equations as

$$\frac{\partial J}{\partial a_{ij}} = 0, \qquad 0 \le i \le n, \quad 0 \le j \le n. \tag{3}$$

In order to avoid ill solution, a singular value decomposition method (SVD) [18] is used to solve the above equations.

In our algorithm, the points with reliable densities should be paid more attention. The variance of ridge distance computed in a point's neighborhood can be used to indicate how reliable the computed density is. The lower the variance is, the more influence the point should have in WLS algorithm. We use the following function to normalize the weight to [0, 1] according to the computed variance, i.e.,

$$w = \exp\left(-\frac{\sigma^2}{8}\right) \tag{4}$$

where w denotes the normalized weight and σ^2 denotes the variance. Experimental results show that this function works well. In order to reduce the computation, those points whose weight is smaller than a certain threshold will be discarded; then, the weighted approximation according to density variance can efficiently decrease the influence of inaccurate density estimation.

As we know, a higher order polynomial can provide a better approximation, but at the same time it will result in a much higher cost of storage and computation. Moreover, a high-order polynomial will be ill behaved on numerical approximation. As to a lower order polynomial, however, it will yield lower approximation accuracy in those regions with high curvature. As a tradeoff, we choose four-order (i.e., $n = 4$) polynomials for the global approximation. The experimental results have shown that they perform well enough for most real fingerprints, while preserving a small cost for storage and computation.

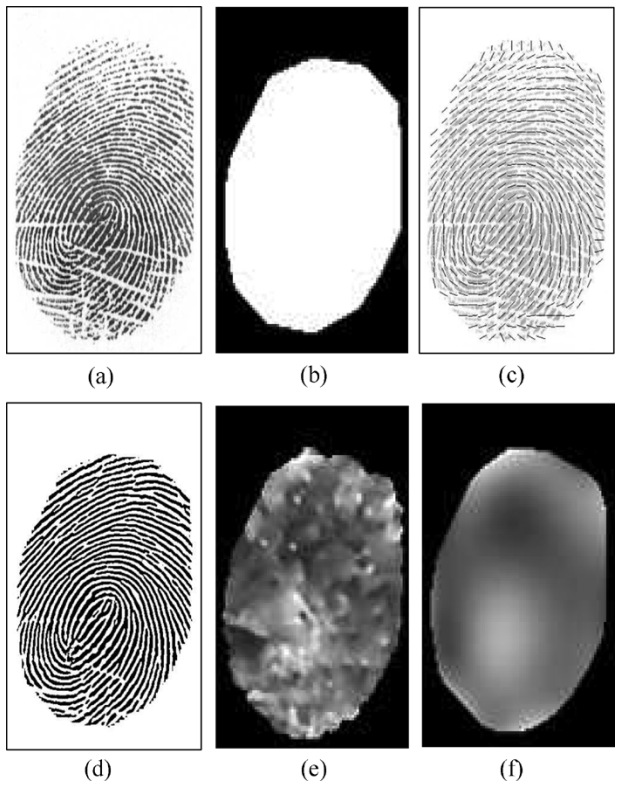

Fig. 4. Results of each step in model-based density map computation: (a) original fingerprint; (b) the effective region recorded using 16-point chain code; (c) orientation field; (d) enhanced fingerprint image; (e) coarse density map and (f) the modeled density map. In (e) and (f), normalized gray-level values are used to indicate the ridge distance.

After approximation, 4 bytes are used to record the minimal value and maximal value of all polynomial's coefficients, respectively. Then, only 50 bytes are needed to save 25 normalized coefficients of the bivariate polynomial (i.e., each coefficient is saved in 2 bytes). As mentioned above, it needs 32 bytes to record the effective region, so the total storage cost for density features is 90 bytes. It is much smaller than the storage cost of the features proposed in [8]–[11] (all of which are larger than 640 bytes). Such a low storage cost guarantees the real applications of density information into match stage.

An example of model-based density map computation with the result of each step is provided in Fig. 4.

III. Fingerprint Matching Using Density Map

In this section, we will utilize the saved density features into the matching stage by combining them with minutiae information. A matching scheme is proposed for density maps between two fingerprints. Then its score is combined with the matching score between two fingerprints' minutiae.

A. Density Map Matching

To compare two density maps reconstructed from saved polynomial parameters, a first step is alignment of these two fingerprints. It can be done in a same way as in conventional fingerprint algorithms, in which the alignment is mainly based on minutiae information [1]–[3], [5]. In our study, we choose the Hough-transform based approach [19], [20] to finish the alignment due to its simplicity.

In the matching step, the correlation between two aligned density maps, A and B, is computed as below. Let C denote the intersection of the two effective regions after alignment, and N is the total number of points in C. The matching score between two density maps of two fingerprints is defined as

$$\epsilon_1(A,B) = \begin{cases} \frac{1}{N}\sum_{(i,j)\in C}|a_{i,j}-b_{i,j}| & N \neq 0 \\ \infty & N = 0. \end{cases} \quad (5)$$

A simple method is further taken to normalize the matching score as

$$\epsilon(A,B) = 1 - \exp\left(-\epsilon_1(A,B)\right). \quad (6)$$

If the matching score in (6) is less than a certain threshold, we say the two density maps are matched.

B. Combination of Density Map Matching and Minutiae Matching

Since fusion of classifiers may allow alleviation of problems intrinsic to individual classifiers, the matching performance could be improved by applying a combination strategy on the output from minutiae-based matching and density map matching. In this part, we try to integrate density map matching and minutiae matching.

A variety of combination rules have been proposed [21], such as product rule, sum rule, max rule, min rule, median rule, and majority voting rule. Jain *et al.* [8], [22], [23] have shown that matching accuracy can be improved by combining "independent" matchers using Neyman-Pearson rule. Since the ridge distance in the neighborhood of minutiae point always has a greater variance, which will lead in a smaller weight in approximation, the effects of minutiae points could be removed greatly. So, we can regard that density map matching and minutiae matching are nearly independent. Then, we decided to use Neyman-Pearson rule for our task of the combination here.

Let s_1 and s_2 denote the scores from the minutiae-based matcher and proposed modeled density map matcher, respectively. Let ω_G denote the genuine class, while ω_I denote the imposter class; then, $p(s_1|\omega_G)$ and $p(s_2|\omega_G)$ are the genuine class-conditional probability density functions for s_1 and s_2, respectively. Similarly, $p(s_1|\omega_I)$ and $p(s_2|\omega_I)$ denote the imposter's. The error rates of two classes are defined as

$$\begin{cases} P_G(e) = \int_{\mathcal{R}_I} p(s_1,s_2|\omega_G)ds_1ds_2 \\ P_I(e) = \int_{\mathcal{R}_G} p(s_1,s_2|\omega_I)ds_1ds_2 \end{cases} \quad (7)$$

where $\Re_G$ and $\Re_I$ denote the distributed region of ω_G and ω_I, respectively. Our goal is to minimize the ω_G's error rate [false rejection rate (FRR)], under a given pre-specified error rate [false acceptance rate (FAR)], i.e., $\varepsilon_0 = P_I(e)$. To do that, we define the fusion score $s(s_1,s_2)$ for s_1 and s_2 as

$$s(s_1,s_2) = \frac{p(s_1,s_2|\omega_G)}{p(s_1,s_2|\omega_I)}. \quad (8)$$

According to the Neyman-pearson rule for a given (s_1^0, s_2^0), the classification rule is as follows:

$$\left(s_1^0,s_2^0\right) \in \begin{cases} \omega_G, & \text{if } s\left(s_1^0,s_2^0\right) > \lambda \\ \omega_I, & \text{otherwise} \end{cases} \quad (9)$$

where λ is the threshold to minimize FRR under a given FAR.

Under the assumption that s_1 and s_2 are statistically independent, the probability density functions $p(s_1,s_2|\omega_G)$ and $p(s_1,s_2|\omega_I)$ can be calculated as

$$\begin{cases} p(s_1,s_2|\omega_G) = p(s_1|\omega_G)p(s_2|\omega_G) \\ p(s_1,s_2|\omega_I) = p(s_1|\omega_I)p(s_2|\omega_I). \end{cases} \quad (10)$$

Then, the key point here is to estimate the probability density functions, i.e., $p(s_1|\omega_G), p(s_2|\omega_G), p(s_1|\omega_I)$, and $p(s_2|\omega_I)$. We tackle this problem by using a Parzen density estimation method on a training set (see [23]). The estimated probability density functions can be saved for global usage.

The ridge density feature might be influenced by elastic distortion and different pressure. But a small distortion cannot produce an evident affection to the matching score between two fingerprints belonging to a same identity, mainly due to the continuity of the density model and matching scheme. Since the proposed density-based matching method is based on minutiae alignment, it may fail to match two fingerprints from a same identity under a large distortion, which is similar with the performance of the minutiae-based matching method. Then it cannot result in additional error by adding density information into the matching stage. The experiments also illustrate the above conclusions, and the results will be listed in the next section.

IV. Experimental Results

Our experiments are conducted on three databases, including the THU database of our lab and two public domain collections FVC2002 DB1 and DB2 [24].

The THU database consists of 6616 fingerprint impressions selected from, which are captured with live-scanners $(\text{image size} = 320 \times 512)$. All these fingerprints are from 827 different fingers, and eight fingerprints per finger. These fingerprint images have different sizes and vary in different qualities. In them, more than 40% of these images are suffering the affection from creases, scars and smudges in the ridges or dryness and blurs of the fingers. The database is randomly divided into two parts: one is used as the training set for the combination scheme, which contains 3200 (400×8) fingerprints, and the other is used as the testing set, which contains 3416 (427×8) fingerprints.

Both DB1 and DB2 from FVC2002 contain 800 fingerprints, i.e., 100 fingers and eight prints for each finger, respectively. These two databases are also used for testing. The FVC2002 database has following features [24]: 1) fingerprints collected in three sessions with at least two weeks time separating each

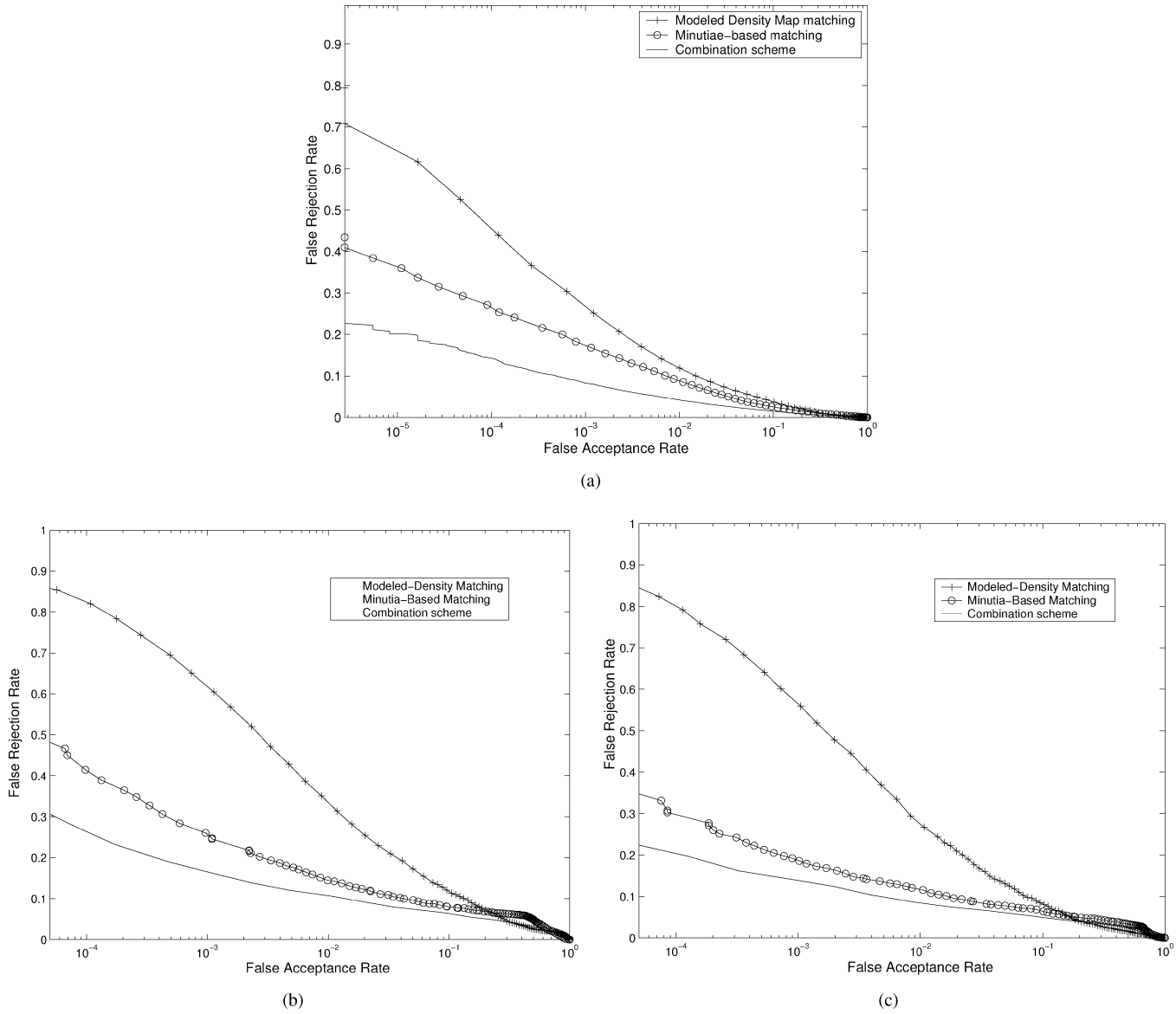

Fig. 5. ROC of three schemes, modeled density map matching, minutiae-based matching and the combination scheme, respectively, on the THU testing database (a), DB1 (b), and DB2 (c), of FVC2002, respectively.

session; 2) no efforts were made to control image quality and the sensor platens were not systematically cleaned; 3) at each session, four impressions were acquired of each of the four fingers of each volunteer; 4) during the second session, individuals were requested to exaggerate displacement (impressions 1 and 2) and rotation (3 and 4) of the finger, not to exceed 35°; and 5) during the third session, fingers were alternatively dried (impressions 1 and 2) and moistened (3 and 4).

For THU database, the number of genuine-matching pairs is $11\,200(C_8^2 \times 400)$ and $11\,956(C_8^2 \times 427)$ for the training set and testing set, respectively. Since the matching number is much larger that that of genuine pairs if we match all imposter pairs, our strategy is randomly choosing two fingerprints from the every eight ones which come from a same finger to form a subset, then, each imposter pair in this subset has to be tested. So, the number of imposter matching in the training set and testing set is $319\,200(C_{400\times 2}^2 - 400)$ and $363\,804(C_{427\times 2}^2 - 427)$, respectively. For DB1 and DB2, the number of genuine-matching pairs is 2800 and that of imposter-matching pairs is 316 800.

We test the independence of minutiae matching and density map matching on the training set. As stated in [23], [26] a correlation coefficient can be used as a measure of diversity between a pair of matchers. A lower correlation always means a higher independence between two matchers and a larger improvement can be obtained by combining these two matchers. In our experiments, we computed the correlation coefficient between minutiae-based matching and modeled density map matching and it is 0.28, 0.24, and 0.29 on THU database, DB1 and DB2, respectively. It is much lower than the correlation coefficients reported in [23], which are all larger than 0.50 between each of three different minutiae-based matching methods and FingerCode-based matching [8]. That means modeled density map can complement with minutiae much better than FingerCode.

We compared two fingerprint recognition systems, i.e., one is singly using minutiae information and the other is the proposed

TABLE I
MATCHING RATES OF TWO SYSTEMS BY USING MINUTIAE-BASED MATCHING SINGLY AND THE PROPOSED COMBINATION METHOD, RESPECTIVELY, USING THE LEAVE-ONE-OUT STRATEGY

Number of best matches	THU Testing Database (200×8 fingerprints)		DB1 (60×8 fingerprints)		DB2 (60×8 fingerprints)	
	minutiae-based	ours	minutiae-base	Ours	minutiae-base	ours
1	0.955	0.988	0.981	0.996	0.969	0.988
2	0.952	0.985	0.982	0.990	0.967	0.984
3	0.944	0.978	0.963	0.983	0.956	0.981
4	0.933	0.969	0.942	0.972	0.946	0.975
5	0.921	0.960	0.918	0.958	0.936	0.968
6	0.910	0.949	0.880	0.934	0.908	0.949
7	0.888	0.930	0.824	0.888	0.853	0.908

algorithm. In these two systems, the information of minutiae part is the same and the only difference lies in density information is added in the proposed algorithm. So, the performances of the two systems can be fairly compared by the final recognition results.

Fig. 5 shows the receiver operating curves (ROC) plotting FAR versus FRR of minutiae matching scheme, modeled density map matching scheme and the combination scheme, on THU testing database, DB1 and DB2, respectively. FRR is defined as the percentage of imposter matches in all genuine pairs. FAR is defined as the percentage of genuine matches in all imposter pairs. From the ROC, we can see that combining the density information with minutiae matching can have a rather excited result, although the performance of singly using density map is far from satisfying. FRR can be reduced a lot by using the combination scheme against the minutiae-based matching only.

Table I shows the matching rates of these two matching schemes (i.e., using the minutiae-based matching scheme and the combination scheme) on three subsets from THU testing database, DB1 and DB2, respectively. The matching rate is defined as the percentage of correct fingerprints (of the same finger) present among the best $n(n = 1, 2, \cdots, 7)$ matches. It shows that the matching rate can also be improved evidently by adding density information.

By analyzing the experimental results, we find the reasons why the performance of combination strategy is better than singly using minutiae matching mainly lie in the following. 1) The poor-quality part in fingerprints may result in spurious minutiae and the spurious minutiae may give negative contribution to the FRR. The modeled density map matching may overcome this problem to some extend by adding some positive contribution. 2) In some cases, two minutiae sets matched well, but the textures of the region are dissimilar. Then it will result in a false match by singly using minutiae matching. But the dissimilarity of texture may lead a negative matching score of modeled density map matching which indicates they are imposters, so the combination matching may give a right result.

Our system is implemented on a Pentium IV 1500-Hz PC computer. Compared with singly using minutiae matching scheme, the computational time of the hybrid algorithm will be a little longer. Additional computation cost for feature extraction is about 0.19 s, and the additional matching time (one-to-one) is less than 0.01 s. It shows a high feasibility to utilize the density map into real applications.

V. CONCLUSION

The density map is important for fingerprint representation. In order to utilize the information into fingerprint recognition systems, we proposed a polynomial model to represent the density map and the model's parameters are saved as a novel kind of feature for the matching stage. The advantages of model-based density map can be summarized as follows. 1) It is a novel feature to represent a kind of global character of a fingerprint. 2) Its storage cost is small enough to guarantee its utility in real applications. 3) It can reduce the effect of sharp variation of ridge distance, and then it is much more robust against noise. 4) There exists little redundancy between it and minutiae representation, so it is suitable to combine density map matching with minutiae matching.

A fingerprint matching based on modeled density map is also developed in this paper, which can be combined with conventional minutiae matching for real applications. Experimental results show that the performance of the proposed algorithm is significantly better than singly using minutiae-based matching, which means the new fingerprint representation combining minutiae and density map provides more information.

ACKNOWLEDGMENT

The authors would like to thank the editor and the anonymous reviewers for their valuable comments and suggestions.

REFERENCES

[1] A. K. Jain, R. Bolle, and S. Pankanti, Eds., *BIOMETRICS: Personal Identification in Networked Society*. New York: Kluwer, 1999.
[2] D. Zhang, *Automated Biometrics: Technologies and Systems*. New York: Kluwer, 2000.
[3] K. Hrechak and J. A. McHugh, "Automated fingerprint recognition using structural matching," *Pattern Recognit.*, vol. 23, pp. 893–904, 1990.
[4] S. Pankanti, S. Prabhakar, and A. K. Jain, "On the individuality of fingerprints," *IEEE Trans. Pattern Anal. Mach. Intell.*, vol. 24, no. 8, pp. 1010–1025, Aug. 2002.
[5] A. Jain, H. Lin, and R. Bolle, "On-line fingerprint verification," *IEEE Trans. Pattern Anal. Mach. Intell.*, vol. 19, no. 4, pp. 302–314, Apr. 1997.
[6] F. Pernus, S. Kovacic, and L. Gyergyek, "Minutiae-based fingerprint recognition," in *Proc. 5th Int. Conf. Pattern Recognition*, Miami Beach, FL, 1980, pp. 1380–1382.

[7] X. Tan and B. Bhanu, "On the fundamental performance for fingerprint matching," in *Proc. IEEE Computer Soc. Conf. Computer Vision and Pattern Recognition*, vol. 2, Jun. 2003, pp. 499–504.
[8] A. K. Jain, S. Prabhakar, L. Hong, and S. Pankanti, "Filterbank-based fingerprint matching," *IEEE Trans. Image Process.*, vol. 9, no. 5, pp. 846–859, May 2000.
[9] A. Ross, A. Jain, and J. Reisman, "A hybrid fingerprint matcher," *Pattern Recognit.*, vol. 36, pp. 1661–1673, 2003.
[10] M. Tico and P. Kuosmanen, "Fingerprint matching using an orientation-based minutia descriptor," *IEEE Trans. Pattern Anal. Mach. Intell.*, vol. 25, no. 8, pp. 1009–1014, Aug 2003.
[11] A. Jin, B. Teoh, D. Ling, and O. T. Song, "An efficient fingerprint verification system using integrated wavelet and Fourier-Mellin invariant transform," *Image Vis. Comput.*, vol. 22, pp. 503–513, 2004.
[12] L. O'Gorman and J. V. Nickerson, "An approach to fingerprint filter design," *Pattern Recognit.*, vol. 22, pp. 28–38, 1989.
[13] R. Cappelli, D. Maio, and D. Maltoni, "Synthetic fingerprint-database generation," in *Proc. 16th Int. Conf. Pattern Recognition*, vol. 3, Aug. 2002, pp. 744–747.
[14] J. Zhou and J. Gu, "A model-based method for the computation of fingerprints' orientation field," *IEEE Trans. Image Process.*, vol. 13, no. 6, pp. 821–835, Jun. 2004.
[15] L. Hong, Y. F. Wan, and A. Jain, "Fingerprint image enhancement: Algorithm and performance evaluation," *IEEE Trans. Pattern Anal. Mach. Intell.*, vol. 20, no. 8, pp. 777–789, Aug. 1998.
[16] Z. M. Kovacs-Vajna, R. Rovatti, and R. Frazzoni, "Fingerprint ridge distance computation methodologies," *Pattern Recognit.*, vol. 33, pp. 69–80, 2000.
[17] P. Whittle, *Prediction and Regulation by Linear Least-Square Methods*. London, U.K.: English Univ. Press, 1963.
[18] *Numerical Recipes in C++: The Art of Scientific Computing*. Cambridge, U.K.: Cambridge Univ. Press, 2002.
[19] G. Stockman, S. Kopstein, and S. Benett, "Matching images to models for registration and object detection via clustering," *IEEE Trans. Pattern Anal. Mach. Intell.*, vol. PAMI-4, pp. 229–241, 1982.
[20] N. K. Ratha, K. Karu, S. Chen, and A. Jain, "Real-time matching system for large fingerprint database," *IEEE Trans. Pattern Anal. Mach. Intell.*, vol. 18, no. 8, pp. 799–813, Aug. 1996.
[21] J. Kittler, M. Hatef, R. P. W. Duin, and J. Matas, "On combining classifiers," *IEEE Trans. Pattern Anal. Mach. Intell.*, vol. 20, no. 3, pp. 226–239, Mar. 1998.
[22] A. Jain, S. Prabhakar, and S. Chen, "Combining multiple matchers for a high security fingerprint verification system," *Pattern Recognit. Lett.*, vol. 20, pp. 1371–1379, 1999.
[23] S. Prabhakar and A. Jain, "Decision-level fusion in fingerprint verification," *Pattern Recognit.*, vol. 35, no. 4, pp. 861–874, 2002.
[24] D. Maltoni, D. Maio, A. K. Jain, and S. Probhaker, *Handbook of Fingerprint Recognition*. New York: Springer-Verlag, 2003.
[25] S. Zhang and K. S. Fu, "A thinning algorithm for discrete binary image," in *Proc. Int. Conf. Computers and Applications*, Beijing, China, 1984, pp. 879–886.
[26] L. I. Kuncheva and C. J. Whitaker, "Measures of diversity in classifiers ensembles and their relationship with the ensemble accuracy," *Mach. Learn.*, vol. 51, pp. 182–207, 2003.

Dingrui Wan was born in 1981. He received the B.S. degree from the Department of Automation, Tsinghua University, Beijing, China, in 2004, where he is currently pursuing the Ph.D. degree.

His research interests are in pattern recognition, computer vision, and intelligent information processing.

Jie Zhou (M'01–SM'04) was born in 1968. He received the B.S. and M.S. degrees from the Department of Mathematics, Nankai University, Tianjin, China, in 1990 and 1992, respectively, and the Ph.D. degree from the Institute of Pattern Recognition and Artificial Intelligence, Huazhong University of Science and Technology (HUST), Wuhan, China, in 1995.

From 1995 to 1997, he was a Postdoctoral Fellow with the Department of Automation, Tsinghua University, Beijing, China. Currently, he is a Full Professor and Assistant Chair with the Department of Automation, Tsinghua University. His research area includes pattern recognition, image processing, computer vision, and information fusion. In recent years, he has authored more than ten papers in international journals and more than 40 papers in international conferences.

Dr. Zhou received the Best Doctoral Thesis Award from HUST; the First Class Science and Technology Progress Award from the Ministry of Education, China; and the Excellent Young Faculty Award from Tsinghua University in 1995, 1998, and 2003, respectively. He is an Associate Editor for the *International Journal of Robotics and Automation*.